

Structural changes and elastic characteristics of permanently densified vitreous B₂O₃Giovanni Carini Jr.,^{1,3} Edmondo Gilioli,² Gaspare Tripodo,¹ and Cirino Vasi³¹*Dipartimento di Fisica, Università di Messina, Viale Ferdinando Stagno d'Alcontres 31, I-98166 Messina, Italy*²*IMEM del C.N.R., Area delle Scienze, I-43010 Parma, Italy*³*IPCF del C. N. R., Sezione di Messina, Viale le Ferdinando Stagno d'Alcontres 37, I-98166 Messina, Italy*

(Received 27 October 2010; revised manuscript received 28 April 2011; published 13 July 2011)

Inelastic light-scattering spectra of normal and permanently densified B₂O₃ glasses were investigated over the frequency range between 6 and 1600 cm⁻¹. Densification from 1826 to 2320 kg/m³ was obtained by loading B₂O₃ glasses in a multianvil apparatus for synthesis at 2 and 4 GPa; they were fused at temperatures between 1400 and 1500 K and then were quenched at those pressures. It is shown that increasing densification gives rise to (i) a growing decrease of the intensity of the strong band at 808 cm⁻¹, ascribed to the breathing vibration of boroxol rings, implying a reduction in the number of rings in the network and (ii) the appearance of a band at 775 cm⁻¹ in the glass compacted at 4 GPa, which is assigned to the vibrations of structural units containing tetrahedral BO₄ groups. The low-frequency Raman scattering includes the boson peak (BP), which dominates the spectra between 10 and 100 cm⁻¹. Densification significantly decreases the intensity of the BP and shifts its position from about 26 cm⁻¹, through 39 cm⁻¹ (2-GPa glass), up to 68 cm⁻¹ (4-GPa glass). These increases are stronger than those expected from the substantial hardening of the elastic continuum: The elastic moduli increase up to about a factor of 5 compared to those of normal glass. These observations imply that densification drives the system toward a structure having a more efficient packing of molecular units, causing substantial variations of the short- and medium-range orders with the formation of boron atoms in the four-fold-coordinated state at a quenching pressure of 4 GPa.

DOI: [10.1103/PhysRevB.84.024207](https://doi.org/10.1103/PhysRevB.84.024207)

PACS number(s): 78.30.Ly, 63.50.Lm

I. INTRODUCTION

The vibrational dynamics of glasses continues to be a very interesting and widely studied topic. In fact, the topological disorder in the glassy structures leads to an excess density in low-energy vibrational states $g(\nu)$ over the Debye contribution, which gives a broad hump in the inelastic neutron- and light-scattering spectra, known as the boson peak (BP) and frequently ascribed to structural correlations over the intermediate-range length scale.¹⁻³ Despite numerous experimental and theoretical studies, the BP as well as other low-frequency anomalies of vibrational properties of glasses associated with low-energy excitations are not yet understood.⁴⁻⁶ An interesting consideration is that the BP appears in the energy range where acoustic phonons have a wavelength on the order of a few nanometers, implying that structural heterogeneities, observed in glasses over the nanometer length scale,⁷ could be responsible for strong scattering of phonons. Recently, interest in this issue has further been stimulated by the finding that the BP arises mainly from transverse vibrational modes associated with defective soft structures of nanometer sizes in the glass.⁸ As suggested from previous experiments,⁹ the size of structural heterogeneities can be determined by the frequency of the BP and the sound velocity in the system.

This prediction opens new methods for the investigation of the origin of the BP because significant changes in the sizes of the structural heterogeneities in a glass are expected by varying its density without altering its stoichiometry. This can be obtained by hot densification of a glass, that is, by quenching the melt of a glass-forming liquid subjected to high pressures (gigapascal range). Since the structure of hot densified glasses reflects one of the supercooled liquids at high pressure at the

glass transition temperature T_g , remarkable modifications of the short- and intermediate-range orders are expected.

An archetype of glassy oxides, such as B₂O₃, permanently hot densified at increasing pressures gave evidence of polymorphism (or better, polyamorphism),¹⁰⁻¹² that is, a transition from low- to high-density amorphous phases characterized by a coordination increase of network forming ions (NFI) from three to four and by significant variations in the intermediate-range order. In particular, very recent studies based on nuclear magnetic resonance (NMR) measurements in hot densified glassy B₂O₃ (Ref. 12) revealed that (i) the fraction of three-fold-coordinated boron atoms (B⁽³⁾) involved in boroxol rings decreases gradually from about 0.78 in the normal glass to about 0.3 in the glass compacted at 5.8 GPa and (ii) four-fold-coordinated boron atoms (B⁽⁴⁾) are absent in glasses compacted below 4 GPa. Boroxol rings (B₃O₆) are the molecular groups formed by connected BO₃ planar triangles, which are the basic units building up the network of normal vitreous B₂O₃.¹³⁻¹⁶ These findings are in contrast with the results of a previous NMR study on hot densified glassy B₂O₃ (Ref. 11), which disclosed (i) a fraction of B⁽³⁾ increasing from about 0.75 in the normal glass to about 0.8 in the glass compacted at 2 GPa, then substantially decreasing to about 0.41 in the one compacted at 6 GPa and (ii) the presence of B⁽⁴⁾ in both compacted glasses, their fraction increasing with the pressure of synthesis.

The present paper reports a study of the low- and high-frequency Raman scatterings having the analysis of the evolution for the BP and the modifications of the short- and medium-range orders as the objectives, which are induced by hot densification of B₂O₃ glasses at 2 and 4 GPa. In particular, the structural changes have been evaluated by a compared analysis of the boroxol breathing mode at 808 cm⁻¹

and the high-frequency multicomponent band between 1200 and 1600 cm^{-1} associated with vibrations involving both the boroxol rings and the residual network of BO_3 units. The results unambiguously show the decrease in boroxol rings with increasing pressure of synthesis and the appearance of tetracoordinated boron atoms only in the glass densified at 4 GPa.

II. EXPERIMENTAL DETAILS

B_2O_3 glasses were prepared by melt quenching using, as a starting material, laboratory reagent 99.999% purity grades of boron oxide isotopically enriched in ^{11}B (99%) because the same samples considered for the present analysis will be used for future experiments of elastic and inelastic neutron-scattering measurements. $^{11}\text{B}_2^{16}\text{O}_3$ powder was heated at 150 °C for 24 h in a N_2 atmosphere in order to reduce any water content. The dehydrated powder was melted in an alumina crucible, and a clear bubble free melt was obtained after 2 h at 1250 °C. The melt was cast into a preheated 250-°C split-steel mold to prepare a glass cylinder about 15-mm long and 6 mm in diameter. The glasses were annealed and were stabilized at ~ 540 K (~ 20 K above their calorimetric glass transition temperature T_g) in a high-purity nitrogen atmosphere and then were cooled and were stored at room temperature. Densification was obtained by loading B_2O_3 glasses in a multianvil high-temperature/high-pressure apparatus for synthesis at 2 and 4 GPa. They were fused under pressure at 1150 °C for about 10 (2-GPa I glass) or 20 min (2-GPa II glass) and at 1200 °C (4-GPa glass) for about 30 min and then were quenched at those pressures. A typical raw sample had a diameter and a length of about 4.5 mm. Both the normal and the compacted samples were clear, transparent, and good optical quality glasses. After the synthesis and also few months later, the densified B_2O_3 glasses were characterized by x-ray diffraction, which did not reveal any sign of crystallization.

The density was measured at room temperature by a Micromeritics AccuPyc 1330 gas pycnometer under helium gas, which had 0.03% accuracy. The densities of normal and densified B_2O_3 glasses are as follows: 1826 kg/m^3 (normal), 2082 kg/m^3 (2 GPa), and 2320 kg/m^3 (4 GPa).

The Raman spectra were performed at room temperature on a double monochromator Jobin Yvon U-1000 and were recorded in 90° scattering geometry in both vertical-vertical (VV) (incident and scattered light is polarized vertical to the scattering plane) and vertical-horizontal (VH) geometry (perpendicular polarizations). The incident light was the 514.5-nm line of an argon-ion laser with power kept below 300 mW along with a polarization scrambler between the sample and the entrance slit of the spectrometer. The accuracy of all stated measurements is within 1 cm^{-1} . To minimize the effect of surface depolarization, the sample surfaces were polished before each run of measurement.

Longitudinal and shear sound waves were obtained by tuning X- and Y-cut quartz crystals at their fundamental frequency. The sample-transducer bonding agent was Apiezon N grease. The sound velocity measurements of longitudinal (v_l) and shear (v_t) waves were performed at 10 MHz and at room temperature by a pulse-echo technique.

III. RESULTS AND DISCUSSION

A. High-frequency Raman scattering

The Raman spectra of normal and permanently densified (at 2 and 4 GPa) $v\text{-B}_2\text{O}_3$ between 6 and 1600 cm^{-1} are shown in Fig. 1 for the VV (polarized) configuration. The Raman scattering was also measured in the VH (depolarized) configuration: The depolarization ratio and the spectral characteristics (frequency and full width at half height) of normal $v\text{-B}_2\text{O}_3$ are in close agreement with those reported by Windisch, Jr. and Risen, Jr. for a glass of $^{11}\text{B}_2^{16}\text{O}_3$ (Ref. 17). The spectra can be divided into two frequency regions: (i) The low-frequency part (below 100 cm^{-1}) characterized by the BP and (ii) the high-frequency part, which is dominated by the very intense and highly polarized band at 808 cm^{-1} , associated with a localized breathing-type vibration of oxygen atoms inside the plain boroxol ring composed of three corner-sharing BO_3 .¹⁷⁻¹⁹ Further vibrational features characterizing the high-frequency region are as follows: (i) the lines below 750 cm^{-1} that reflect an optical-like motion of atoms inside the basic units building up the network^{18,19} and (ii) the multicomponent band between 1200 and 1600 cm^{-1} , which is assigned (a) to vibrations of oxygen atoms bridging two boroxol rings (1202 cm^{-1}) or a boroxol ring to the network of BO_3 units (1253 cm^{-1}) and (b) to the boron motion in chainlike segments (1323 cm^{-1}) or in the residual network (1457 cm^{-1}) of connected BO_3 units.^{16,17} It has been shown that the 1457- cm^{-1} band remains quite constant up to temperatures well above the melting point, implying that the residual network of BO_3 units is unaffected by temperature.¹⁶ The comparison of the spectra reveals that densification gives rise to significant changes in both the low- and the high-frequency regions: (i) The BP shows a relevant decrease in the intensity and a substantial increase in the frequency ω_{BP} , which shifts from about 26 cm^{-1} in normal glass, through 39 cm^{-1} (2-GPa glass), to about 68 cm^{-1} (4-GPa

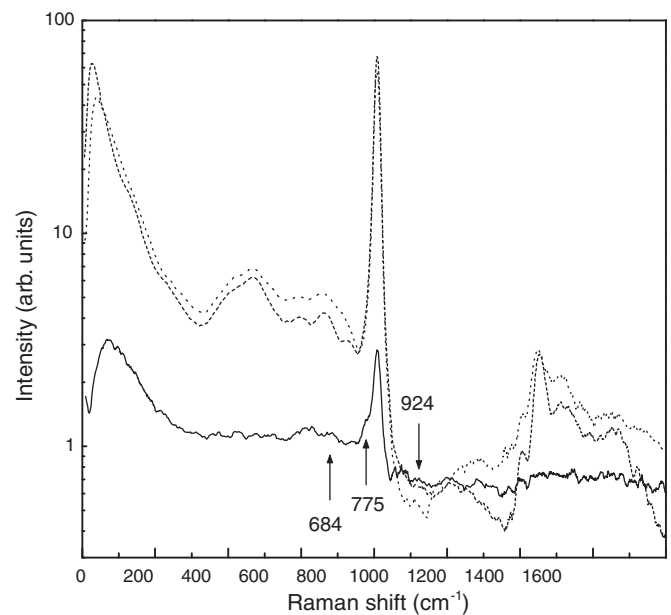


FIG. 1. Room-temperature Raman spectra of densified B_2O_3 glasses for VV polarization: dashed line, normal glass; dotted line, 2-GPa glass; solid line, 4-GPa glass.

glass); (ii) the band at 808 cm^{-1} and the four components of the multicomponent band between 1200 and 1600 cm^{-1} keep their positions, exhibiting a slight decrease in the intensity over a flat background due to a small contribution from fluorescence in normal and 2-GPa glasses. Quite differently, we note a marked decrease in the overall intensity in 4-GPa glass and, most importantly, the unquestionable appearance of a shoulder in the 808-cm^{-1} band at about 775 cm^{-1} . Smaller bands are also observed at 684 cm^{-1} , 924 cm^{-1} , and in the region around 500 cm^{-1} . Since in borate glasses with low alkali oxide content,²⁰ the band observed at 770 cm^{-1} along with weaker features at 666 cm^{-1} , 930 cm^{-1} , and in the 500-cm^{-1} regions has been ascribed to vibrations in pentaborate units, two boroxol rings linked by a tetracoordinated boron atom, we assign the 775-cm^{-1} shoulder observed in 4-GPa glass to vibrations in structural units containing $\text{B}^{(4)}$. The formation of BO_4 groups implies changes due to densification in the chemical bonding characterizing the glassy network.

Except for this striking evidence in 4-GPa glass, the vibrational motion associated with boroxol rings and BO_3 units appears to be weakly affected by densification, leading to the conclusion that these molecular groups preserve the main characteristics of their conformations. Taking the close similarity between the high-frequency spectra into account, it is expected that the line at 1457 cm^{-1} ascribed to BO_3 units building up the residual network should be temperature and also pressure independent, allowing us to use it as a reference for evaluating the variation in the boroxol-ring fraction with densification. We will apply the following procedure, which has been previously proposed for determining the changes of high-frequency modes in B_2O_3 glasses with different thermal histories.²¹ First, from each spectrum, a background corresponding to the value of the scattered intensity in the high-frequency region has been subtracted, where no molecular vibrations are revealed. Afterward, for each sample, the integrated intensities in the 808-cm^{-1} mode including the shoulder at 775 cm^{-1} for 4-GPa glass and in the different lines forming the multicomponent high-frequency band have been evaluated by a Lorentzian fit. In particular, a multicomponent fit has been used to decompose the latter band in four separate peaks, whose spectral characteristics for the normal and compacted glasses are in agreement with the results of a previous analysis performed in a glass of $^{11}\text{B}_2^{16}\text{O}_3$.¹⁷ The results of the fits for 2-GPa I glass are shown in Fig. 2, and the values of the integrated intensities I_{ω_i} are reported in Table I. It is worth noting that, for a more accurate and quantitative comparison, the values obtained for densified $v\text{-B}_2\text{O}_3$ have been reduced by the ratio between the densities of compacted and normal glasses (about 1.14 and 1.27 for 2- and 4-GPa glasses, respectively) in order to account for a larger average number of particles characterizing the scattering volume. The ratio $R = I_{808}/I_{1457}$ (Table I) decreases substantially with increasing quenching pressure and points to a decreasing fraction of boroxol rings with growing densification. Since the fraction of boroxol rings changes during the cooling process from about 0.2 at 1300 K up to about 0.6 at 300 K in $v\text{-B}_2\text{O}_3$ at the atmospheric pressure P_{amb} (Ref. 16), it results that the application of high pressures strongly hinders the transformation of BO_3 -chain-like segments in rings, resulting

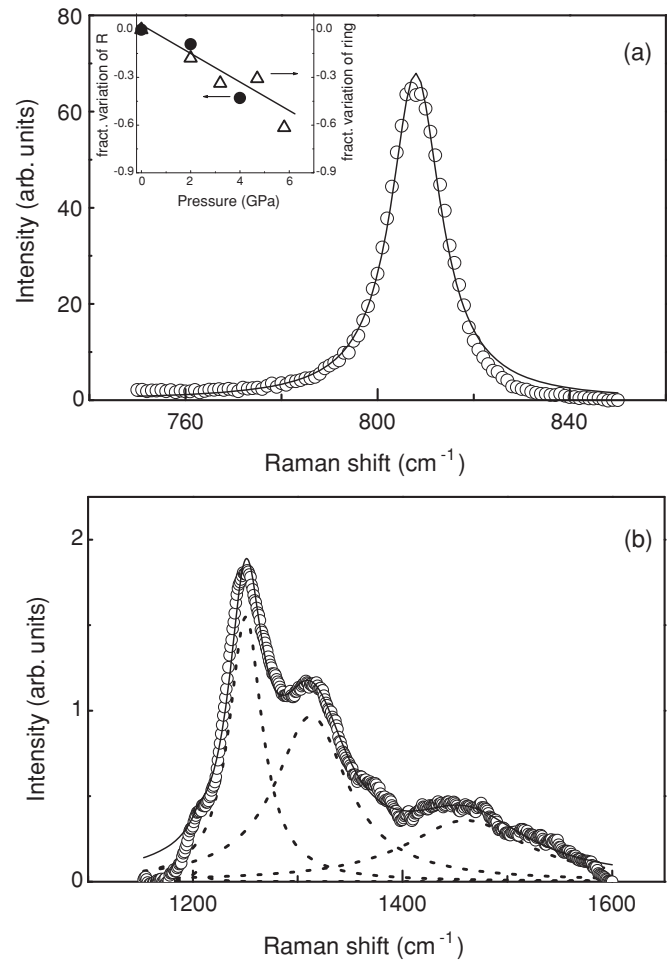


FIG. 2. Room-temperature Raman spectra in VV polarization of (a) the 808-cm^{-1} mode and (b) the multicomponent band between 1100 and 1600 cm^{-1} of 2-GPa glass. Dotted and solid lines show the single Lorentzian fits and their addition, respectively. Inset of (a) shows the fractional variations of the ratio $R = I_{808}/I_{1457}$ (solid symbols, present Raman measurements) and of the boroxol ring content (open symbols, NMR data taken from Ref. 12) vs quenching pressure obtained in densified B_2O_3 glasses. Solid line is a guide for eyes only.

in a ratio R at 4 GPa about 40% lower than that of the normal glass. It is worth emphasizing that the two different values of the ratio obtained for 2-GPa I and 2-GPa II glasses are surely a consequence of the different exposition times at high temperatures. Accounting for the massive size of the samples, it is believed that the shortest time (10 min) was not sufficient

TABLE I. Integrated intensities in the bands at 775 , 808 cm^{-1} , and in the lines forming the multicomponent band in the range between 1200 and 1600 cm^{-1} for normal and densified $v\text{-B}_2\text{O}_3$.

B_2O_3 glasses	I_{775}	I_{808}	I_{1202}	I_{1253}	I_{1323}	I_{1457}	$R_{808/1457}$
Normal		1615.6	2.9	98.0	160.9	114.2	14.15
2-GPa I		1233	1.78	68.9	120.2	87.3	14.13
2-GPa II		2240	2.71	156.6	387.7	174.4	12.85
4 GPa	33.2	53.1	0.7	8.5	29.4	10.6	8.14

to permit the attainment of the full thermodynamic equilibrium of the liquid under high pressure.

The present findings are in close agreement with the results of a NMR study by Brazhkin *et al.*¹² They revealed that the number of boroxol rings in v -B₂O₃, hot densified at pressures ranging between 2 and 5.8 GPa, decreases with increasing pressure and, in addition to this, densification assists the formation of B⁽⁴⁾ only for pressures $P > 3.2$ GPa. The fractional variations of the ratio R , given by $\frac{R(P) - R(P_{\text{amb}})}{R(P_{\text{amb}})}$, and of the content of boroxol rings derived by NMR analysis are reported as a function of the pressure of synthesis in the inset of Fig. 2(a) and exhibit very good agreement. It results that the application of pressure up to 4 GPa in the liquid phase gives rise to substantial variations of the connectivity of the glassy network, obtained by rapid cooling of the melt under pressure. Pressure limits the formation of boroxol rings during the quenching process but also causes modification of the chemical bonding giving rise to tetracoordinated boron atoms. This is because the quenching process under pressure drives the system toward a structure having a more efficient packing of the molecular units in order to fit to the lower volume available to it.

B. Low-frequency Raman scattering and elastic characteristics

Since the four components of the multicomponent band are associated with vibrations of all the units forming the whole glassy network, the low-frequency Raman spectra (6–300 cm⁻¹) of normal and densified v -B₂O₃ have been normalized by its total integrated intensity. The normalized and reduced Raman spectra of all the investigated glasses at room temperature are shown in Fig. 3. It results that densification gives rise to a relevant increase in the BP frequency ω_{BP} , from 26 to 68 cm⁻¹, while significantly decreasing its intensity. The reduced Raman intensity I_R is proportional to the reduced density of low-energy vibrational states $g(\omega)/\omega^2$,

$$I_R(\omega) = \frac{I_{\text{exp}}}{\omega [n(\omega, T) + 1]} = C(\omega) \frac{g(\omega)}{\omega^2} \quad (1)$$

It has been proved, in fact, that the absence of translation symmetry gives rise to a Stokes component of the low-frequency Raman intensity I_{exp} , which reflects the product between the light-vibration coupling coefficient $C(\omega)$ and $g(\omega)$, also accounting for the Bose-Einstein population factor $n(\omega) = (e^{\hbar\omega/k_B T} - 1)^{-1}$.²² The complexity of the vibrational characteristics of disordered systems affects both functions $C(\omega)$ and $g(\omega)$. Over the frequency region of BP, $C(\omega)$ exhibits a linear frequency dependence and $g(\omega)$ shows a behavior exceeding the Debye prediction.^{23,24}

An interesting result is given by plotting the curves of I_R scaled by the maximum intensity I_{BP} of the BP vs the ratio $\frac{\omega}{\omega_{\text{BP}}}$, Fig. 3(b). Despite the significant variations observed in the amplitude and the position of the BP with increasing density, all the scaled curves overlap showing a nearly identical shape for $\frac{\omega}{\omega_{\text{BP}}} \geq 0.7$. At lower frequencies, the curve of 4-GPa glass deviates from the common behavior exhibited by normal and 2-GPa glasses. It is believed that the observed deviation reflects the substantial variation of the short- and medium-range orders induced by modification of the chemical bonding in this system. A further contribution to be considered for an

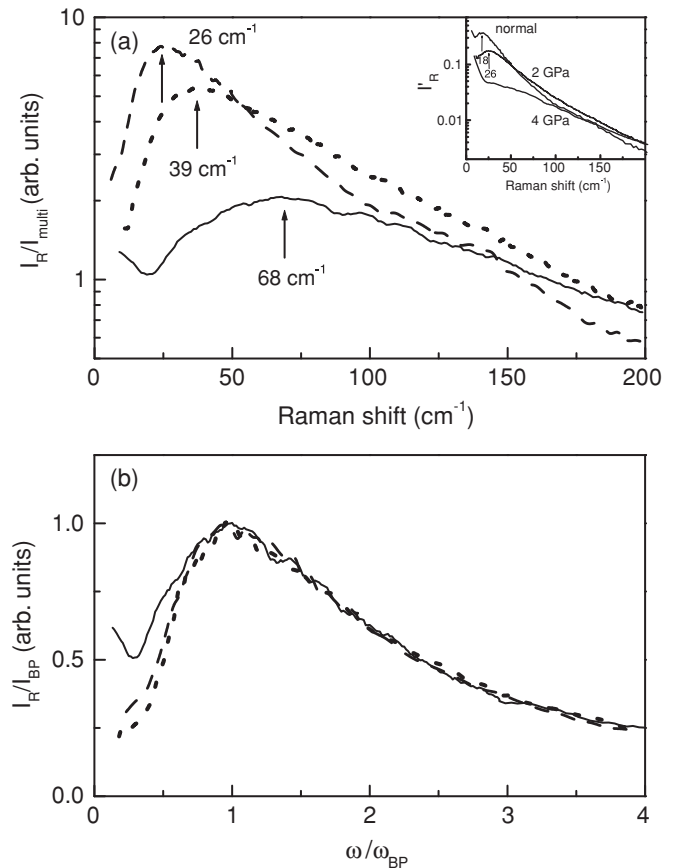


FIG. 3. (a) Reduced Raman intensity I_R normalized by the integrated intensity of the high-frequency multiband I_{multi} of normal and densified B₂O₃ glasses: dashed line, normal glass; dotted line, 2-GPa glass; solid line, 4-GPa glass. Inset of (a) shows I_R/ω , denoted as I'_R of the same glasses. (b) Comparison of the BP of normal and densified B₂O₃ glasses, plotted as I_R/I_{BP} vs $\omega/\omega_{\text{BP}}$.

accurate evaluation of the low-frequency tail of the BP is the quasielastic light-scattering excess, which regulates the Raman scattering in glasses at frequencies below about 10–20 cm⁻¹. It is strongly temperature dependent and due to the coupling between the light and the thermally activated fast relaxations.²⁵ For its evaluation, it is necessary to perform Raman-scattering measurements over a wide range of temperatures down to about 10 K, and such kinds of experiments are, at present, in progress. The invariance of the $\frac{I_R}{I_{\text{BP}}}$ curves, at least in normal and 2-GPa glasses, seems to indicate the existence of a low-energy vibrational dynamics underlying the BP where all the modes, extended and quasilocalized, are coupled and are hybridized, resulting in an overall distribution whose spectral shape does not change with densification.

As discussed above, the BP is associated with additional vibrational modes besides the acoustic phonons, which originate in the amorphous structures. It is believed that all the related experimental findings could have a common origin: An excess density in vibrational states arising from localization of low-energy excitations ascribed to the presence of a characteristic length in an amorphous system. This length has been variously interpreted^{9,26,27} in order to justify the sharp onset of quasilocalized vibrational excitations involving an intermediate length scale and causing a deviation from the

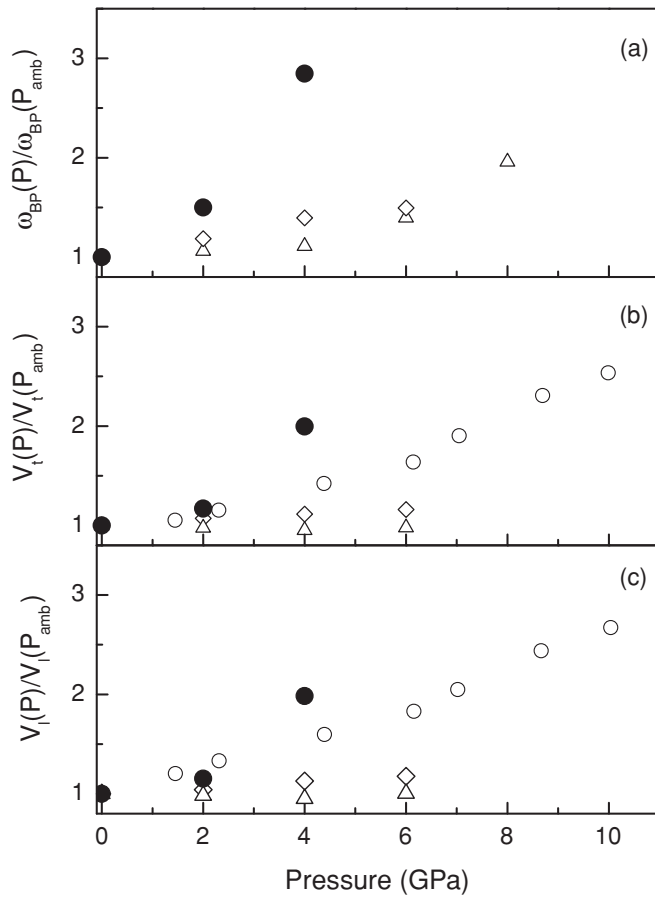


FIG. 4. Comparison between the BP frequency ω_{BP} and the sound velocities normalized at the ambient pressure values and plotted vs the quenching pressure in glasses compacted at temperatures above (hot) and below (cold) T_g : (a) \bullet , ω_{BP} in B_2O_3 (hot, present results); \diamond , GeO_2 (cold, Ref. 31); Δ , SiO_2 (cold, Ref. 32); (b) \bullet , shear sound velocity $v_t(P)$ in B_2O_3 (hot, present results); \diamond , GeO_2 (cold, Ref. 31); Δ , SiO_2 (cold, Ref. 32); and \circ , B_2O_3 (*in situ* measurements, Ref. 33); (c) \bullet , longitudinal sound velocity $v_l(P)$ in B_2O_3 (hot, present results); \diamond , GeO_2 (cold, Ref. 31); Δ , SiO_2 (cold, Ref. 32); and \circ , B_2O_3 (*in situ* measurements, Ref. 33).

behavior expected for the usual acoustic phonons. The relevant length scale ξ_b can be estimated as²⁷

$$\xi_b = \frac{Sv_D}{c\omega_0} \quad (2)$$

where ω_0 (expressed in cm^{-1}) is the frequency of the BP maximum in the real reduced density of low-energy vibrational states $g(\omega)/\omega^2$, v_D is the average Debye velocity, c is the velocity of light, and S ($=0.65$) is a mean shape factor of the structural domain having ξ_b as a relevant size. The Debye velocity is given by $\frac{3}{v_D^3} = \frac{1}{v_l^3} + \frac{2}{v_t^3}$. In the absence of neutron-scattering data on densified glasses, we use the alternative procedure described below, which allows us to obtain a rough evaluation of ω_0 with the knowledge of the reduced Raman intensity I_R . Since I_R is given by Eq. (1), we assume that the linear-frequency dependence of $C(\omega)$ observed in normal v - B_2O_3 (Ref. 23) is also maintained in the compacted glasses so that the spectral shape of $g(\omega)/\omega^2$ can be determined

by the ratio I_R/ω . The corresponding curves show maxima at $\omega_0 = 18 \text{ cm}^{-1}$ for normal glass and $\omega_0 = 26 \text{ cm}^{-1}$ for 2-GPa glass (inset of Fig. 3(a)), while a continuously decreasing curve without any defined maximum is obtained for 4-GPa glass. The latter behavior surely reflects the substantial structural changes, which severely affect the frequency dependence of $C(\omega)$ and prevent the determination of ω_0 in this glass. It is worth noting that the value in normal glass is in very close agreement with that derived by the effective $g(\omega)/\omega^2$ determined by inelastic neutron-scattering measurements.²⁸ Using these values together with those of sound velocities measured at room temperature in both glasses (Table II) in Eq. (2), one obtains $\xi_b = 2.45 \text{ nm}$ for normal glass and $\xi_b = 1.98 \text{ nm}$ for the densified one. The significant decrease of ξ_b with increasing density is in agreement with the predictions of a theoretical model,²⁹ which relates the BP to a characteristic length ξ defining the sizes of soft regions with nonaffine elastic displacements embedded in amorphous solids. ξ marks the length scale below which the classical elastic continuum theory loses its predictive validity in evaluating the low-frequency vibrational modes, which are characterized by an excess over the Debye prediction determined by contributions from the soft regions. Increasing density should decrease the sizes of the heterogeneities driving the system toward a phase characterized by a growing mechanical stability.^{29,30} In addition to this, the decreasing ξ_b proves that the changes of low-energy vibrational dynamics are not accounted for by the transformations of the elastic continuum because the variation of the BP frequency is larger than that of the average sound velocity.

The hardening of the elastic continuum increases with increasing densification leading to bulk $B(= \rho v_l^2 - \frac{4}{3}G)$ and shear, $G(= \rho v_t^2)$ moduli, which exhibit a sharp jump of about a factor of 5 in 4-GPa glass (Table II). This is because the tetracoordinated boron atoms represent a unique source for the connectivity (defined as the number of bridging bonds per NFI) and the associated stiffening of the borate network. The variations in ω_{BP} and sound velocities vs quenching pressure in hot densified glassy B_2O_3 are considerably larger than those revealed in glasses compacted at temperatures below T_g ,^{31,32} Fig. 4. The sound velocities, in particular, appear to follow the behaviors observed by *in situ* measurements on vitreous B_2O_3 at 273 K over a wide range of applied pressures,³³ even if with a quite higher value in the 4-GPa glass. This is probably due to the fact that, by *in situ* measurements, the coordination change in NFIs from trigonal to tetrahedral has been inferred to start at a compression pressure of about 11 GPa, the original state of the three-coordinated vitreous B_2O_3 being recovered on decompression at 3 GPa. These results show that changes in structure and vibrational dynamics of glasses retrieved under pressure from temperatures above T_g are substantial and are much more effective than those in pressure-quenched glasses at temperatures below T_g . It is worthwhile to note that the pressure dependence of the ultrasonic velocities and moduli in compacted B_2O_3 glasses differs markedly from those observed in tetrahedrally bonded glasses, such as SiO_2 and GeO_2 . These systems show a minimum over the pressure range between ambient pressure and 5 GPa either by *in situ* measurements^{34,35} or in cold densified glasses;³² the latter data being reported in

TABLE II. Parameters of normal and densified B_2O_3 glasses. Room-temperature values of the density ρ , longitudinal (v_l) and shear (v_t) sound velocities, Debye sound velocity (v_D), bulk (B), and rigidity (G) moduli.

B_2O_3 glasses	ρ (kg m $^{-3}$)	v_l (m s $^{-1}$)	v_t (m s $^{-1}$)	v_D (m s $^{-1}$)	B (GPa)	G (GPa)
Normal	1826	3242	1830	2036	10.66	6.12
2 GPa	2082	3737	2141	2379	16.30	9.54
4 GPa	2320	6393 ^a	3653	4059	53.54	30.96

^aThis value of v_l has been obtained by assuming $\frac{v_l}{v_t} = 1.75$, that is, the same value determined in 2-GPa glass.

Figs. 4(b) and 4(c). The observed minima have been interpreted in terms of structural rearrangements under pressure between different crystallinelike polymorphs.

The present observations imply that the hardening of the elastic continuum is not sufficient to account for the shift to higher frequencies of the BP. This is evidenced by the comparison in Fig. 4 between the normalized ratios of ω_{BP} (which increases by up to about a factor of 3) and the sound velocities (by up to about a factor of 2), disclosing a possible different nature of the additional low-energy excitations over the ordinary elastic waves. Densification at elevated pressures in B_2O_3 glasses causes modifications of the short- and medium-range orders, associated with the formation of more packed groups of atoms, which shift the whole distribution of underlying vibrational modes to higher frequencies but preserving its spectral shape up to quenching pressures of about 2 GPa.

IV. CONCLUSIONS

Raman-light-scattering measurements performed at room temperature over the frequency range between 6 and 1600 cm^{-1} in B_2O_3 glasses, permanently compacted by melt quenching under high pressures (gigapascal range), reveal that the structural variations of the glassy network due to densification concern both the short- and the medium-range orders. Analysis of the high-frequency region shows that the main vibrational band at 808 cm^{-1} , associated with vibrations of boroxol rings, preserves its frequency but decreases substantially in intensity with increasing density from 1826 kg/m^3

(normal v - B_2O_3) up to 2320 kg/m^3 (4-GPa glass). In addition, the appearance of a band at 775 cm^{-1} has been revealed in the densest glass, which is assigned to vibrations of groups containing tetracoordinated boron atoms. These observations imply that increasing density of the glass is associated with the decrease of the fraction of boroxol rings and to the enhancement of the network connectivity by variations in the chemical bonding. Melt quenching under pressure up to 4 GPa of B_2O_3 hinders the transformation of BO_3 -chain-like segments in rings during the cooling process, driving the system toward a glassy structure having a more efficient packing of the molecular units. Low-frequency Raman scattering below 150 cm^{-1} evidences that the BP decreases in magnitude and increases in frequency from 26 cm^{-1} to 68 cm^{-1} with increasing density. The determination of a characteristic length calculated from the BP position and the sound velocities unambiguously proves that the observed variations in the low-energy vibrational dynamics cannot be accounted for by the modifications of the elastic continuum, which experiences a substantial hardening with an enhancement of the elastic moduli by up to a factor of 5. The results of this analysis disclose an important reduction in the size of structural domains, which are believed to be the main source of additional soft vibrations giving rise to the BP.

ACKNOWLEDGMENT

The authors want to thank Gaetano Di Marco (IPCF del C. N. R., Messina, Italy) for helpful discussions and his support in measuring the density of compacted glasses.

¹U. Buchenau, H. M. Zhou, N. Nücker, K. S. Gilroy, and W. A. Phillips, *Phys. Rev. Lett.* **60**, 1318 (1988).

²A. P. Sokolov, U. Buchenau, W. Steffen, B. Frick, and A. Wischniewski, *Phys. Rev. B* **52**, R9815 (1995).

³A. Fontana, F. Rossi, G. Carini, G. D'Angelo, G. Tripodo, and A. Bartolotta, *Phys. Rev. Lett.* **78**, 1078 (1997).

⁴B. Rufflè, D. A. Parshin, E. Courtens, and R. Vacher, *Phys. Rev. Lett.* **100**, 015501 (2008).

⁵K. Niss, B. Begen, B. Frick, J. Ollivier, A. Beraud, A. Sokolov, V. N. Novikov, and C. Alba-Simionesco, *Phys. Rev. Lett.* **99**, 055502 (2007).

⁶G. Monaco and V. M. Giordano, *Proc. Natl. Acad. Sci. USA* **106**, 3650 (2009).

⁷E. Duval, A. Mermet, and L. Saviot, *Phys. Rev. B* **75**, 024201 (2007).

⁸G. D'Angelo, G. Carini, C. Crupi, M. Koza, G. Tripodo, and C. Vasi, *Phys. Rev. B* **79**, 014206 (2009).

⁹E. Duval, A. Boukenter, and T. Achibat, *J. Phys.: Condens. Matter* **2**, 10227 (1990).

¹⁰V. V. Brazhkin and A. G. Lyapin, *J. Phys.: Condens. Matter* **15**, 6059 (2003).

¹¹S. K. Lee, K. Mibe, Y. Fei, G. D. Cody, and B. O. Mysen, *Phys. Rev. Lett.* **94**, 165507 (2005).

¹²V. V. Brazhkin, I. Farnan, K.-i. Funakoshi, M. Kanzaki, Y. Katayama, A. G. Lyapin, and H. Saitoh, *Phys. Rev. Lett.* **105**, 115701 (2010).

¹³P. J. Bray, *J. Non-Cryst. Solids* **73**, 19 (1985).

¹⁴C. Joo, U. Werner-Zwanziger, and J. W. Zwanziger, *J. Non-Cryst. Solids* **261**, 282 (2000).

¹⁵R. E. Youngman *et al.*, *Science* **269**, 1416 (1995).

- ¹⁶A. K. Hassan, L. M. Torrel, L. Borjesson, and H. Doweidar, *Phys. Rev. B* **45**, 12797 (1992).
- ¹⁷C. F. Windisch Jr. and W. M. Risen Jr., *J. Non-Cryst. Solids* **48**, 307 (1982).
- ¹⁸F. L. Galeener, G. Lucovsky, and J. C. Mikkelsen Jr., *Phys. Rev. B* **22**, 3983 (1980).
- ¹⁹R. A. Barrio, F. L. Castillo-Alvarado, and F. L. Galeener, *Phys. Rev. B* **44**, 7313 (1991).
- ²⁰B. N. Meera and J. Ramakrishna, *J. Non-Cryst. Solids* **159**, 1 (1993).
- ²¹N. V. Surovtsev, J. Wiedersich, A. E. Batalov, V. N. Novikov, M. A. Ramos, and E. Rossler, *J. Chem. Phys.* **113**, 5891 (2000).
- ²²R. Shuker and R. W. Gammon, *Phys. Rev. Lett.* **25**, 222 (1970).
- ²³N. V. Surovtsev and A. P. Sokolov, *Phys. Rev. B* **66**, 054205 (2002).
- ²⁴A. Fontana *et al.*, *J. Phys.: Condens. Matter* **19**, 205145 (2007).
- ²⁵G. Carini, M. Federico, A. Fontana, and G. A. Saunders, *Phys. Rev. B* **47**, 3005 (1993).
- ²⁶S. R. Elliot, *Europhys. Lett.* **19**, 201 (1992).
- ²⁷A. Mermet, N. V. Surovtsev, E. Duval, J. F. Jal, J. Dupuy-Philon, and A. J. Dianoux, *Europhys. Lett.* **36**, 277 (1996).
- ²⁸D. Engberg, A. Wischniewski, U. Buchenau, L. Borjesson, A. J. Dianoux, A. P. Sokolov, and L. M. Torell, *Phys. Rev. B* **58**, 9087 (1998).
- ²⁹F. Léonforte, R. Boissiere, A. Tanguy, J. P. Wittmer, and J.-L. Barrat, *Phys. Rev. B* **72**, 224206 (2005); F. Léonforte, A. Tanguy, J. P. Wittmer, and J.-L. Barrat, *Phys. Rev. B* **73**, 055501 (2006).
- ³⁰L. E. Silbert, A. J. Liu, and S. R. Nagel, *Phys. Rev. Lett.* **95**, 098301 (2005).
- ³¹L. Orsingher *et al.*, *Philos. Mag.* **88**, 3907 (2008).
- ³²M. Zanatta *et al.*, *Phys. Rev. B* **81**, 212201 (2010).
- ³³J. D. Nicholas, R. E. Youngman, S. V. Sinogeikin, J. D. Bass, and J. Kieffer, *Phys. Chem. Glasses* **44**, 249 (2003); J. Nicholas, S. Sinogeikin, J. Kieffer, and J. Bass, *Phys. Rev. Lett.* **92**, 215701 (2004).
- ³⁴C.-s. Zha, R. J. Hemley, Ho-k. Mao, T. S. Duffy, and C. Meade, *Phys. Rev. B* **50**, 13105 (1994).
- ³⁵J. Hertling, S. Baessler, S. Rau, G. Kasper, and S. Hunklinger, *J. Non-Cryst. Solids* **226**, 129 (1998).